remote sensing

Supplementary Materials:

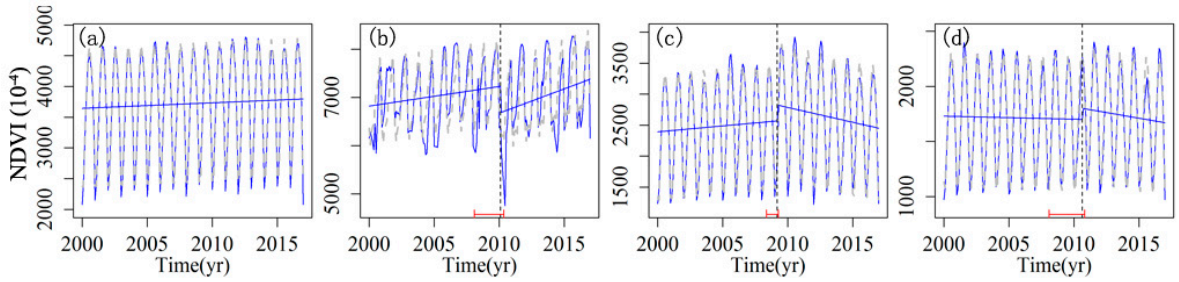

Figure S1. Four types of trend shifts in vegetation greenness on the entire Tibetan Plateau (**a**), OA1 zone (**b**), IC1 zone (**c**), and IIC2 zone (**d**).

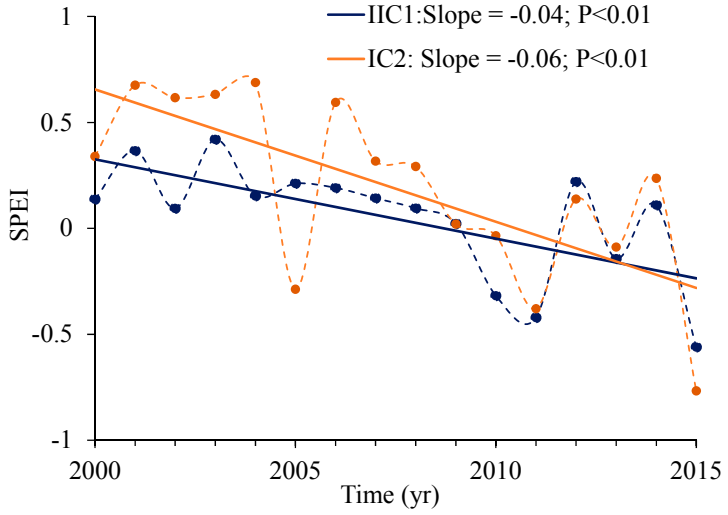

Figure S2. Inter-annual variations of the Standardized Precipitation-Evapotranspiration Index (SPEI) within growing season in the southwestern Tibetan Plateau.

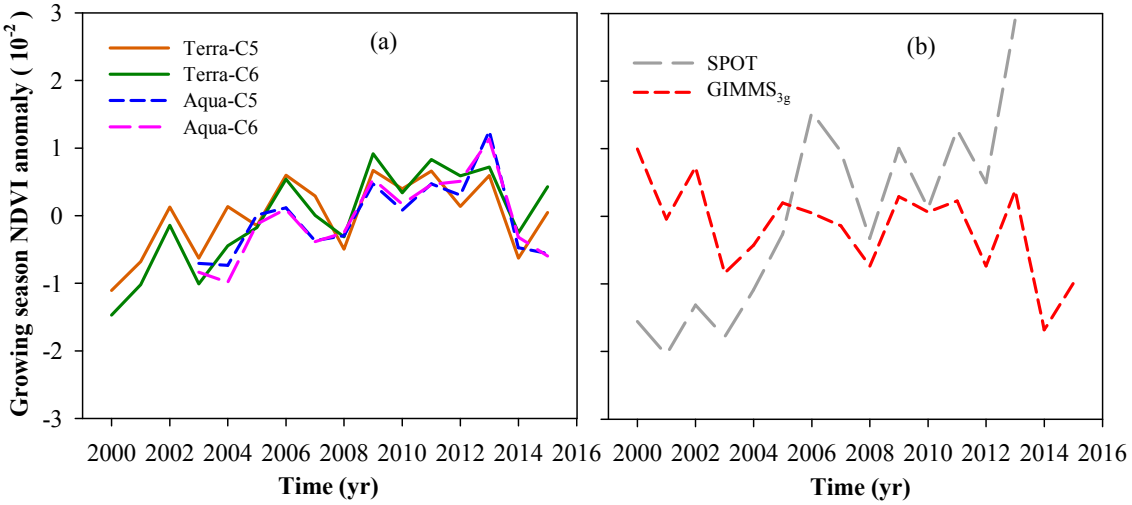

Figure S3. Comparison of growing season NDVI (GNDVI) in vegetated areas on the Tibetan Plateau based on MODIS (**a**), and SPOT-VGT and GIMMS3g (**b**).

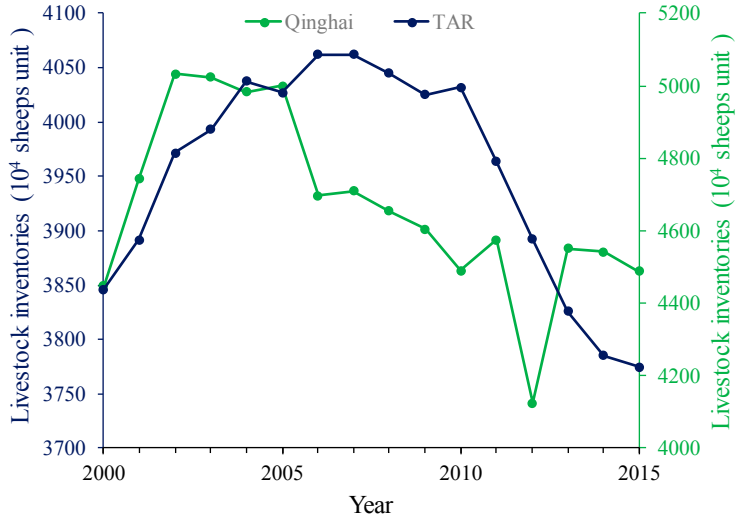

Figure S4. Variation in livestock inventories in Qinghai Province and Tibet Autonomous Region (TAR) between 2000 and 2015.

Text S1. Consistencies and Differences among Inter-Annual Variations of NDVI Data Derived from MODIS and GIMMS3g

The magnitude and patterns of vegetation change on the TP in recent studies are debated, largely due to data uncertainties. Thus, when developing conclusions about the direction, magnitude, and even drivers of vegetation dynamics on the TP, it is particularly important to evaluate differences amongst the multiple datasets [1,2]. Here, we focused on comparing the consistencies and differences among inter-annual variations of NDVI data derived from Terra-MODIS and GIMMS$_{3g}$ since 2000, and NDVI data derived from Aqua-MODIS and SPOT-VGT were used to clarify the performance of those three products (Table S1). It is noteworthy that although NDVI time series derived from SPOT-VGT and GIMMS$_{3g}$ are subject to inconsistencies due to sensor shifts between platforms [3], this issue is not relevant to MODIS NDVI data [2]. Moreover, Aqua-MODIS acquired data two years later than Terra-MODIS and might suffer from less sensor degradation [2,4]; for this reason, several studies therefore used NDVI time series from MODIS Aqua as reference datasets [3,5].

Table S1. Information on the five NDVI data sets used in Text S1.

Dataset	Dataset Source	Spatial resolution	Temporal resolution	Period	Reference
MODIS Terra-C5 (MOD13A2)	https://ladsweb.modaps.eosdis.nasa.gov	1 × 1 km	16 d	2000–2015	[6]
MODIS Aqua-C5 (MYD13A2)	https://ladsweb.modaps.eosdis.nasa.gov	1 × 1 km	16 d	2003–2015	[6]
MODIS Aqua-C6 (MYD13A2)	https://ladsweb.modaps.eosdis.nasa.gov	1 × 1 km	16 d	2003–2015	[7]
GIMMS$_{3g}$	https://ecocast.arc.nasa.gov/data/pub/gimms/3g.v1/	1/12°×1/12°	15 d	1982–2015	[8]
SPOT-VGT	http://www.vito-eodata.be	1 × 1 km	10 d	2000–2013	[9]

At the regional level, the area-averaged GNDVI derived from MODIS Terra-C6 significantly increased on the TP during 2000–2015 (0.0011 year^{-1}, $p < 0.001$), whereas the corresponding GNDVI from Terra-C5 did not conform to such a trend (0.0005 year^{-1}, $p = 0.08$; Figure S3 and Table S2). At the same time, the inter-annual variations in GNDVI based on Terra-C6 were more acceptable agreement with Aqua (i.e., Aqua-C5 and Aqua-C6) than those based on Terra-C5 on the TP for the overlapping period of 2003 to 2015 (Figure S3 and Table S3). These results are in line with the previous study at the global scale [2]. We also found that the GNDVI anomalies based on Terra C5 before and after 2007

were higher and lower, respectively, than their counterparts based on Terra-C6 (Figure S3), likely because Terra-C5 NDVI were influenced by sensor degradation [4,5], especially subsequent to 2007 [2].

The significantly increasing trend of GNDVI from SPOT-VGT is also consistent with that from Terra-C6 (Figure S3). However, $GIMMS_{3g}$ GNDVI decreased significantly during 2000–2015 (–0.0007 $year^{-1}$, $p < 0.05$, Figure S3; Table S2). Although a similar negative trend has also been reported in previous studies on the TP based on GIMMS NDVI [10–12], those trends have proved to be insignificant likely due to the shorter temporal coverage. Furthermore, the correlation coefficient in GNDVI between $GIMMS_{3g}$ and Terra-C6 (Aqua-C6) was relatively low as compared with that between Terra-C6 and Aqua-C6 (Table S3). These results suggest that inter-annual variations in GNDVI based on $GIMMS_{3g}$ were not particularly consistent with their counterparts based on Terra-C6.

Table S2. Summary statistics on growing season NDVI (GNDVI) changes based on MODIS Terra (C5 and C6) and $GIMMS_{3g}$ on the Tibetan Plateau between 2000 and 2015.

Vegetation index	Terra-C5	Terra-C6	$GIMMS_{3g}$
Slope (10^{-2} yr^{-1})	0.05	0.11	-0.07
p	0.08	<0.001	0.046
$+^a$ (%)	61.73	70.37	36.71
$-^b$ (%)	38.27	29.63	63.29
$++^c$ (%)	16.43	23.47	9.79
$--^d$ (%)	6.68	3.64	20.47

Abbreviations: $+^a$ percentage of greening area exhibiting a linear trend greater than zero; $-^b$ percentage of browning area exhibiting a linear trend less than zero; $++^c$ percentage of significantly greening area ($p < 0.05$); $--^d$ percentage of significantly browning area ($p < 0.05$).

Table S3. Correlation coefficients for growing season NDVI (GNDVI) based on MODIS and $GIMMS_{3g}$ on the Tibetan Plateau over the overlapping period of 2003 to 2015.

	Terra-C5	Terra-C6	Aqua-C5	Aqua-C6	$GIMMS_{3g}$
Terra C5	1	0.84***	0.68*	0.63*	0.80***
Terra C6		1	0.77**	0.81***	0.53
Aqua C5			1	0.98***	0.68*
Aqua C6				1	0.57*
$GIMMS_{3g}$					1

Abbreviations: *** $P < 0.001$; ** $P < 0.01$; * $P < 0.05$.

Spatially, GNDVI from both Terra-C6 and Terra-C5 increased in most eastern areas of the TP but decreased in the south-central and southwest TP during 2000–2015 (Figure S5a, b). However, Terra-C6 GNDVI showed greening trends over 70% of vegetated area (23.47% significantly with $p < 0.05$) on the TP, whereas that based on Terra-C5 comprised 61.73% (16.43% significantly with $p < 0.05$; Table S2). We further found that around 69% of the vegetated areas of TP were characterized by either a larger greening trend or a reduced browning trend when calculations were based on Terra-C6 data compared with Terra-C5 (Figure S5c). Specifically, in the eastern TP, most browning areas observed using Terra-C5 data disappeared when calculations were based on Terra-C6, while greening areas observed using Terra-C5 became greener (Figure S5a–c). Conversely, about 11% of vegetated areas characterized by a trend towards browning based on Terra-C5, mainly in the southwestern part of the TP, exhibited a larger browning trend when calculations were based on Terra-C6. Notably, about 7% of the vegetated areas with significant greening trend identified based on Terra-C6 ($p < 0.05$), mainly in the northeast of the TP, were not evident in Terra-C5. Meanwhile, about 3% of vegetated areas with significant browning trend ($p < 0.05$) identified based on Terra-C5 in the southwest TP

were also not evident in Terra-C6 (Figure S5a–c, Table S2). These results are consistent with the early finding that widely browning trends based on Terra-C5 NDVI are not evident in Terra-C6 at the global scale [2].

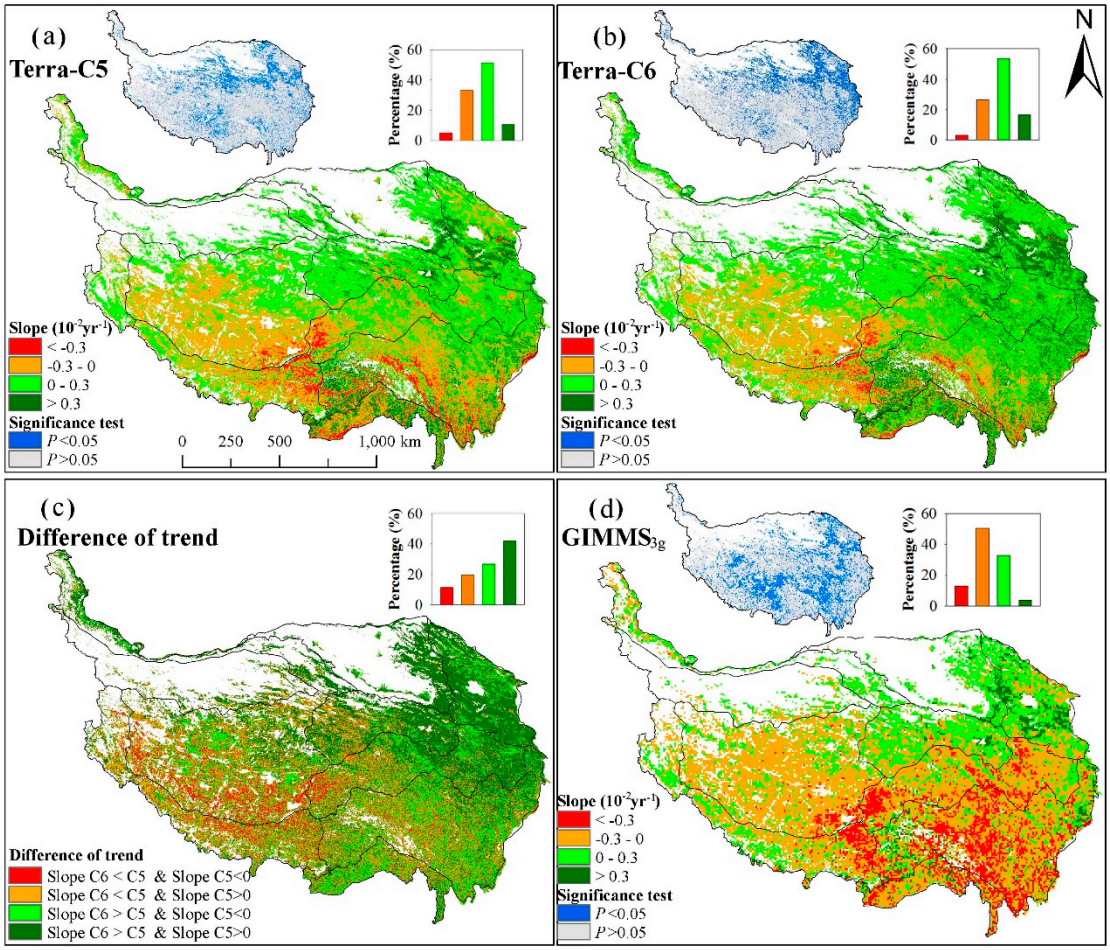

Figure S5. Spatial differences in the growing season NDVI (GNDVI) over the Tibetan Plateau (TP) during 2000-2015 based on (**a**) Terra-C5, (**b**) Terra-C6, and **(d)** GIMMS$_{3g}$. Panel (**c**) shows the differences between Terra-C6 and Terra-C5. The inset bar charts show the frequency distribution of trends corresponding to the legend of the map in each panel.

Compared to Terra-C6 GNDVI, however, GIMMS$_{3g}$ GNDVI exhibited different spatial patterns in the trend of vegetation changes, with 63.29% browning areas (20.47% significantly with $p < 0.05$, Figure S5b, d, Table S2). It is noteworthy that large portions of browning areas in the southeast TP detected by GIMMS$_{3g}$ were not evident in GNDVI based on Terra-C6, while only 36.71% of vegetated areas were characterized by greening trends (9.79%, significant at $p< 0.05$), mainly in the northeast TP. Xu et al. [13] also found that most vegetated area in the western TP were characterized by insignificant correlations between the GIMMS$_{3g}$ NDVI, and SPOT-VGT NDVI during 1998–2013. Similar disagreements between GIMMS NDVI and MODIS NDVI have also been reported for other regions, such as the Sahel and Sudanian zones in Africa [1] and Central Europe [14]. Those conflicting results likely due to the fact that GIMMS NDVI suffer from low data quality, because GIMMS sensors were not originally designed for monitoring vegetation and have been frequently shifted [3] and near-infrared bands of GIMMS were influenced by atmospheric water vapor variation [15,16].

Based on the above analysis, GNDVI based on Terra-C6 might more reliably reflect spatiotemporal changes in the vegetation growth on the TP since 2000 than these based on Terra-C5 and GIMMS$_{3g}$, and GNDVI derived from Terra-C5 and GIMMS$_{3g}$ might underestimate the greening trend on the TP due to the impacts of sensor shifts or degradation.

References

1. Fensholt, R.; Rasmussen, K.; Nielsen, T.T.; Mbow, C. Evaluation of earth observation based long term vegetation trends—Intercomparing NDVI time series trend analysis consistency of Sahel from AVHRR GIMMS, Terra MODIS and SPOT VGT data. *Remote Sens. Environ.* **2009**, *113*, 1886–1898, doi:10.1016/j.rse.2009.04.004.
2. Zhang, Y.; Song, C.; Band, L.E.; Sun, G.; Li, J. Reanalysis of global terrestrial vegetation trends from MODIS products: Browning or greening? *Remote Sens. Environ.* **2017**, *191*, 145–155, doi:10.1016/j.rse.2016.12.018.
3. Tian, F.; Fensholt, R.; Verbesselt, J.; Grogan, K.; Horion, S.; Wang, Y. Evaluating temporal consistency of long-term global NDVI datasets for trend analysis. *Remote Sens. Environ.* **2015**, *163*, 326–340, doi:10.1016/j.rse.2015.03.031.
4. Lyapustin, A.; Wang, Y.; Xiong, X.; Meister, G.; Platnick, S.; Levy, R.; Franz, B.; Korkin, S.; Hilker, T.; Tucker, J.; et al. Scientific impact of MODIS C5 calibration degradation and C6+ improvements. *Atmos. Meas. Tech.* **2014**, *7*, 4353–4365, doi:10.5194/amt-7-4353-2014.
5. Wang, D.; Morton, D.; Masek, J.; Wu, A.; Nagol, J.; Xiong, X.; Levy, R.; Vermote, E.; Wolfe, R. Impact of sensor degradation on the MODIS NDVI time series. *Remote Sens. Environ.* **2012**, *119*, 55–61, doi:10.1016/j.rse.2011.12.001.
6. Huete, A.; Didan, K.; Miura, T.; Rodriguez, E.P.; Gao, X.; Ferreira, L.G. Overview of the radiometric and biophysical performance of the MODIS vegetation indices. *Remote Sens. Environ.* **2002**, *83*, 195–213, doi:10.1016/S0034-4257(02)00096-2.
7. Didan, K.; Munoz, A.B.; Solano, R.; Huete, A. MODIS Vegetation Index User's Guide (MOD13 Series); Version 3.0; University of Arizona: Tucson, AZ, USA, 2015.
8. Pinzon, J.; Tucker, C. A Non-Stationary 1981–2012 AVHRR NDVI3g Time Series. *Remote Sens.* **2014**, *6*, 6929–6960, doi:10.3390/rs6086929.
9. Toté, C.; Swinnen, E.; Sterckx, S.; Clarijs, D.; Quang, C.; Maes, R. Evaluation of the SPOT/VEGETATION Collection 3 reprocessed dataset: Surface reflectances and NDVI. *Remote Sens. Environ.* **2017**, *201*, 219–233, doi:10.1016/j.rse.2017.09.010.
10. Shen, M.; Piao, S.; Jeong, S.; Zhou, L.; Zeng, Z.; Ciais, P.; Chen, D.; Huang, M.; Jin, C.; Li, L.Z.X.; et al. Evaporative cooling over the Tibetan Plateau induced by vegetation growth. *Proc. Natl. Acad. Sci. USA* **2015**, *112*, 9299–9304, doi:10.1073/pnas.1504418112.
11. Tao, J.; Zhang, Y.; Dong, J.; Fu, Y.; Zhu, J.; Zhang, G.; Jiang, Y.; Tian, L.; Zhang, X.; Zhang, T.; et al. Elevation-dependent relationships between climate change and grassland vegetation variation across the Qinghai-Xizang Plateau. *Int. J. Climatol.* **2015**, *35*, 1638–1647, doi:10.1002/joc.4082.
12. Pang, G.; Wang, X.; Yang, M. Using the NDVI to identify variations in, and responses of, vegetation to climate change on the Tibetan Plateau from 1982 to 2012. *Quatern. Int.* **2016**, *44*, 87–96, doi:10.1016/j.quaint.2016.08.038.
13. Xu, H.; Wang, X.; Yang, T. Trend shifts in satellite-derived vegetation growth in Central Eurasia, 1982–2013. *Sci. Total Environ.* **2017**, *579*, 1658–1674, doi:10.1016/j.scitotenv.2016.11.182.
14. Kern, A.; Marjanović, H.; Barcza, Z. Evaluation of the Quality of NDVI3g Dataset against Collection 6 MODIS NDVI in Central Europe between 2000 and 2013. *Remote Sens.* **2016**, *8*, 955, doi:10.3390/rs8110955.
15. Yu, Z.; Wang, J.X.; Liu, S.R.; Sun, P.S.; Liu, W.G. Inconsistent NDVI trends from AVHRR, MODIS, and SPOT sensors in the Tibetan Plateau. In Proceedings of the 2013 Second International Conference on Agro-Geoinformatics (Agro-Geoinformatics), Fairfax, VA, USA, 12–16 August 2013; pp. 97–101.
16. Cihlar, J.; Tcherednichenko, I.; Latifovic, R.; Li, Z.; Chen, J. Impact of variable atmospheric water vapor content on AVHRR data corrections over land. *IEEE Trans. Geosci. Remote. Sens.* **2001**, *39*, 173–180, doi:10.1109/36.898679.